Output Feedback Control and Its Application to a Flexible Spacecraft

Yoon-Gyeoung Sung* and Hae-Ho Joo*

* School of mechanical engineering, Yeungnam University, Kyungbuk, South Korea

ABSTRACT

An output feedback control (OFC) is presented for a linear stochastic system with known disturbance and applied to a flexible spacecraft for the reduction of residual vibration while allowing the natural deflection during operation. By converting the tracking problem into the regulator problem, the OFC minimizes the expected value of a guadratic objective function composing of error states which always remain on the intersection of sliding hypersurfaces. For the numerical evaluation with a flexible spacecraft, a large slewing maneuver strategy is devised with a tracking model for nominal trajectory and a start-coast-stop strategy for economical maneuver in conjunction with the input shaping technique. The performance and efficacy of the proposed control scheme are illustrated with the comparison of different maneuver strategies.

Keywords : Nonlinear Control, Input Shaping, Vibration Reduction, and Kalman Filtering

1. Introduction

In the future generation of flexible spacecraft, the control system design will be a challenging problem because of their special dynamic characteristics which include a large number of significant elastic modes with very small inherent damping, inaccuracies in the knowledge of system parameters, and nonlinear effects. The control methods are related with multi-input, multi-output (MIMO) configuration. As a result, it is natural to use an optimal formulation to design a controller. However, stringent stability and robustness are required due to the space operation. In order to satisfy these requirements, many algorithms have been proposed by employing optimal control, adaptive control, sliding-mode control(SMC), etc.

Sliding-mode control has been used extensively in robotics [1], in which state information is readily available. Slotine proposed the boundary layer concept to reduce the chattering problem by introducing a linear function within the switching region. In the application of SMC to flexible structures, Oz and Mostafa investigated a switching mechanism, stability, interaction with unmodeled dynamics, and the chattering problem with general nonlinear systems. They determined that the chattering issue is not the main obstacle of the application of SMC, but truncation effects are. Young and Ozguner combined SMC with a frequency weighted optimal formulation [4] to reduce the chattering due to rapid switching logic. Sinha and Miller proposed a optimal SMC with Kalman filter to reject stochastic broadband torque disturbances. As a matter of fact, Utkin initially developed the SMCs for multi-variable cases by taking an optimal cost functional. It is possible to combine SMC with an estimator as long as state estimation is asymptotically convergent to the true states [6]. However, an estimator-based SMC has not been adequately addressed

In the paper, an output feedback controller (OFC) is, firstly, presented for a linear stochastic system with known disturbances In the following sections, it analyzes the dynamics of closed-loop system and discusses the constant optimal gain selection of sliding hypersurfaces. The robustness and interaction by unmodeled dynamics is considered. Secondly, in the numerical application of the OFC to the SCOLE

(Spacecraft Control Laboratory Experiment) model, a tracking model is presented with arbitrary influence vector which is chosen by the control system designer. A maneuver strategy are discussed for efficient control implementation in conjunction with the input shaping technique. For the worst scenario to the control scheme, the extreme case with no damping effect is discussed for the performance of the OFC.

2. Output Feedback Control

Consider a linear stochastic system with known disturbances

$$\dot{z}(t) = Az(t) + Bu(t) + Lw(t) + D(t) \tag{1}$$

$$y(t) = Cz(t) + v(t) \tag{2}$$

where state vector $z(t) \in \mathbf{R}^k$, input vector $u(t) \in \mathbf{R}^m$, and output vector $y(t) \in \mathbf{R}^l$. The $D(t)$ contains known disturbances which can be nonlinear functions. It is assumed that (A,B) and (A,C) are controllable and observable, respectively. The plant disturbance vector $w(t)$ and the sensor noise vector $v(t)$ contain independent white-noise processes with zero mean as their elements. Their covariance matrices can be defined as

$$E[w(t)w(\tau)^T] = Q\delta(t-\tau) \tag{3}$$

$$E[v(t)v(\tau)^T] = R\delta(t-\tau) \tag{4}$$

where $\delta(t-\tau)$ is the Dirac delta function. The estimator dynamics for state estimation can be expressed as

$$\dot{\hat{z}}(t) = A\hat{z}(t) + Bu(t) + D(t) + K_f[y(t) - C\hat{z}(t)] \tag{5}$$

where the Kalman gain K_f is obtained by

$$K_f = P, C^T R^{-1} \tag{6}$$

$$\dot{P} = PA^T + AP + Q - PC^T R^{-1} CP \tag{7}$$

If the prescribed configuration vector $z^*(t)$ is considered, the configuration error vector can be expressed as

$$z_e(t) = \hat{z}(t) - z^*(t) \tag{8}$$

Introducing $\hat{z}(t) = z_e(t) + z^*(t)$ into Eq (5), the error dynamics is expressed in terms of the error state vector $x_e(t)$.

$$\dot{z}_e(t) = Az_e(t) + Bu(t) + D(t) + K_f[y(t) - Cz_e(t)] - \dot{z}^*(t) \tag{9}$$

The m hypersurfaces passing through the origin of the error state-space are defined as

$$s_i(t) = g_i^T z_e(t) \qquad i = 1, 2, \cdots, m \tag{10}$$

The control consists of a *reaching phase*, in which the system moves from its initial position in the state space to the sliding surface, and a *sliding phase*, in which it moves along the sliding surface to the origin. The sliding surface *attractivity condition* is typically defined as

$$s_i(t)\,\dot{s}_i(t) \le 0, \qquad i = 1, 2, \cdots, m \tag{11}$$

The attractivity condition and the error dynamics Eq. (9) yield the equivalent controller defined as the solution of $\dot{s}_i(t) = 0$ $(i = 1, 2, \cdots, m)$:

$$u_{eq}(t) = -(GB)^{-1} G[(A - K_f C)\hat{z}(t) + K_f y(t) + D(t) - \dot{z}^*(t)] \tag{12}$$

where $G = [g_1, g_2 \cdots g_m]$. From Eq. (10), the sliding surface is written as

$$S(t) = Gz_e(t) \tag{13}$$

where $S(t) = [s_1(t), s_2(t) \cdots s_m(t)]^T$.

In fact, the equivalent control is an ideal sliding motion on S(0)=0. In order to satisfy the reaching conditions, a switching logic is used for the realization of a smooth sliding motion. In practice, it can be approximated by the reaching controls arbitrarily closely within the limitations of the control switching devices which are related to an infinite switching frequency of controls about the ideal sliding motion. As a result, it becomes a nonideal sliding motion which results in chattering motion. In the practical applications of classical SMC for controlling flexible systems, the chatter phenomenon can excite the unmodeled flexible modes. In this paper, a global asymptotic reaching technique [2, 3] is employed to guarantee convergence without an overshooting problem in the sliding region, so that the overall maneuver is accomplished smoothly. The control law is chosen as

$$u(t) = u_{eq}(t) - (GB)^{-1} P_s S(t) \tag{14}$$

where $P_s = \nu I^{m \times m}$ is selected. As a result, using Eq. (12), Eq. (13) and Eq. (14), the output feedback control law is expressed as

$$u(t) = -(GB)^{-1}[G(A - K_f C)\hat{z}(t) + P_s G z_e(t) + GK_f y(t) + GD(t) - G\dot{z}^*(t)] \tag{15}$$

Notice that the control law includes the direct feedback of the output, estimated states, and tracking trajectory.

3. Analysis and Gain Selection of OFC

In the section, the dynamics in the closed-loop control system is investigated. The optimal gain selection of sliding hypersurface is, then, discussed. Lastly, the robustness is considered for chattering isssue.

3.1 Dynamics of Closed-Loop System

The behaviors of the closed-loop system and estimator can be investigated by defining the estimation error.

$$\bar{z}(t) = z(t) - \hat{z}(t) \tag{16}$$

Using Eq. (1) and Eq. (5), the error dynamics is expressed as

$$\dot{\bar{z}}(t) = (A - K_f C)\bar{z}(t) + Lw(t) - K_f v(t) \tag{17}$$

In terms of $\bar{z}$. Eq. (15) can be written as

$$\begin{aligned} u(t) = -(GB)^{-1}[\, & G(A - K_f C) + GK_f C - P_s G z(t) \\ & - G(A - K_f C) - P_s G]\bar{z}(t) + GK_f v(t) \\ & + GD + P_s G z^*(t) - G\dot{z}^*(t)] \end{aligned} \tag{18}$$

Substituting Eq (18) into Eq. (1), the closed-loop dynamics can be expressed as

$$\begin{aligned} \dot{z}(t) = {} & [A - \Omega A - B(GB)^{-1}P_s G]z(t) \\ & + [\Omega(A - K_f C) - B(GB)^{-1}P_s G]\bar{z}(t) \\ & + Lw(t) - \Omega K_f v(t) - B(GB)^{-1}P_s G z^*(t) \\ & + \Omega \dot{z}^*(t) \end{aligned} \tag{19}$$

where $\Omega = B(GB)^{-1}G$. The closed-loop dynamics are driven by estimation error, noises, and tracking commands. Now, the augmented system of Eq. (17) and Eq. (19) is given as

$$\begin{aligned} \begin{Bmatrix} z(t) \\ \dot{\bar{z}}(t) \end{Bmatrix} = {} & \begin{bmatrix} A - \Omega A + \Gamma & \Omega(A - K_f C) - \Gamma \\ 0 & A - K_f C \end{bmatrix} \begin{Bmatrix} z(t) \\ \bar{z}(t) \end{Bmatrix} \\ & + \begin{bmatrix} L & -\Omega K_f \\ L & -K_f \end{bmatrix} \begin{Bmatrix} w(t) \\ v(t) \end{Bmatrix} + \begin{Bmatrix} -\Gamma x^*(t) + \Omega \dot{z}^*(t) \\ 0 \end{Bmatrix} \end{aligned} \tag{20}$$

where $\Gamma = B(GB)^{-1}P_s G$.

Since the augmented system is block triangular, the eigenvalues are those of $A - \Omega A + \Gamma$ and $A - K_f C$. It is shown that $A - \Omega A + \Gamma$ is the closed-loop plant matrix for full-state feedback problem. As a result, the eigenvalue separation principle holds so that the controller and estimator can be independently designed.

Lemma 3.1: The m eigenvalues of $A - \Omega A + B(GB)^{-1}P_s G$ are decided by $-P_s$ matrix and the remaining k-m eigenvalues can be arbitrarily placed in the S-plane by a proper selection of G since the system (A,B) is controllable.

The proof of *Lemma 3.1* can be presented by the manner of the article by Utkin (1992). Let the columns of a matrix Q_1 consist of basis vectors of the null space of B^T. The coordinate transformation is defined by

$$\eta(t) = M z_e(t) \tag{21}$$

where the matrix M is composed as

$$M = \begin{bmatrix} Q_1 \\ B \end{bmatrix} \tag{22}$$

By substituting Eq. (21) into Eq. (1) and ignoring noises, the transformed equation can be expressed as

$$\dot{\eta}(t) = \bar{A}\eta(t) + \bar{B}u(t) + \bar{D} \tag{23}$$

where

$$\begin{aligned} \bar{A} &= MAM^{-1} \\ \bar{B} &= MB \\ \bar{D} &= MD \end{aligned} \tag{24}$$

Since the matrix M consists of the orthogonal basis of B^T, the first k-m rows of $\bar{B}$ are zero. Therefore, the vector $\eta(t)$ is partitioned such that $\eta_1(t)$ is k-m vector and $\eta_2(t)$ is m vector. The partitioned dynamic equation can be presented as

$$\dot{\eta}_1(t) = A_{11}\eta_1(t) + A_{12}\eta_2(t) + D_1(t) \tag{25}$$

$$\dot{\eta}_2(t) = A_{21}\eta_1(t) + A_{22}\eta_2(t) + B_r u(t) + D_2(t) \tag{26}$$

Then, $S(t)$ can be written as

$$\bar{S}(t) = \eta_2(t) + K_s \eta_1(t) \tag{27}$$

For a full-state feedback problem, the gain G is obtained by equating Eq. (13) with $\bar{S}$ as

$$G = [K_s,\ I^m]\ M \tag{28}$$

Substituting Eq. (27) into Eq. (25) and using global reaching technique [2], the system dynamics for full-state feedback problem can be presented as

$$\begin{aligned} \begin{Bmatrix} \dot{\eta}_1(t) \\ \dot{\bar{S}}(t) \end{Bmatrix} = {} & \begin{bmatrix} A_{11} - A_{12}K_s & A_{12} \\ 0 & -P_s \end{bmatrix} \begin{Bmatrix} \eta_1(t) \\ \bar{S}(t) \end{Bmatrix} \\ & + \begin{Bmatrix} D_1(t) \\ 0^{m\times 1} \end{Bmatrix} \end{aligned} \tag{29}$$

Since the closed-loop system matrix for full-state

feedback problem is $A-\Omega A+B(GB)^{-1}P_sG$ and the eigenvalues remain unchanged under similarity transformation, the eigenvalues of $A-\Omega A+B(GB)^{-1}P_sG$ are k-m eigenvalues from $A_{11}-A_{12}K_s$ and m eigenvalues from $-P_s$. In sliding surface, $\eta_2=-K_s\eta_1$ eigenvalues of $A_{11}-A_{12}K_s$ can be arbitrarily placed in the S plane by proper selection of K_s [6]. In the analysis of the closed-loop dynamics, the feedback term for the attitude control is not considered due to the negligible coordinate.

3.2 Optimal Gain of Sliding Hypersurfaces

As implied in the derivation of the control law, the tracking problem is reduced to the regulator problem with full-state feedback by taking $z_e(t)=\hat{z}(t)-z^*(t)$. The idea can be used for the decision of the matrix G which minimizes the quadratic objective function:

$$J=\int_0^\infty z_e^T(t)Q_sz_e(t)\,dt \tag{30}$$

where Q_s is symmetric and positive semidefinite. Using Eq.(21),

$$J=\int_0^\infty \eta^T(t)(M^{-1})^TQ_sM^{-1}\eta(t)dt \tag{31}$$

With the property of similarity transformation, the matrix $(M^{-1})^TQ_sM^{-1}$, which is symmetric and positive semidefinite defined as

$$(M^{-1})^TQ_sM^{-1}=\begin{Bmatrix} Q_1 & N \\ N^T & R \end{Bmatrix} \tag{32}$$

Hence, the performance index can be expressed as

$$J=\int_0^\infty\{\eta_1^T(t)Q_1\eta_1(t)+\eta_2^T(t)R\eta_2(t)+2\eta_1^T(t)N\eta_2(t)\}dt \tag{33}$$

As a standard linear quadratic problem Eq. (33), the optimal feedback gain matrix [8] is written as

$$K_s=(R)^{-1}[A_{12}^T\ ,\ P_2+N^T] \tag{34}$$

where

$$0=P_2(A_{11}-A_{12}R^{-1}N^T)+(A_{11}^T-NR^{-1}A_{12}^T)P_2-P_2A_{12}R^{-1}A_{12}^TP_2+Q_1-NR^{-1}N^T \tag{35}$$

The optimal gain G is obtained by substituting Eq. (34) into Eq. (28). However, there is a question as to whether or not the choice of G minimizes the stochastic objective function similar to the deterministic case. As long as the objective function meets linear quadratic Gaussian problem, the optimality of J in a stochastic sense is guaranteed [9].

3.3 Robustness of Reaching Dynamics

Due to the chattering issue of the sliding-mode controller, it utilizes the globally asymptotic reaching technique based on an ideal linear model. In order to evaluate the robustness of the technique in the presence of non-ideal effects such as parameter uncertainty, time-varying dynamics and internal or external disturbances, one can check that the ideal sliding surface is guaranteed.

Eq. (1) with non-ideal effects can be expressed as

$$\dot{z}(t)=Az(t)+Bu(t)+\Delta f \tag{36}$$

where Δf accounts for all nonideal effects. If a controller is designed with a linear dynamic model with globally asymptotic reaching technique, the control law can be obtained as

$$u(t)=-(GB)^{-1}[P_sG+GA]z(t) \tag{37}$$

Now, if the control law is applied to Eq.(36), the *reaching condition* can be written as

$$\begin{aligned} S^T(t)\,\dot{S}(t)&=(Gz(t))^T[GAz(t)+GBu(t)+G\Delta f]\\ &=(Gz(t))^T[-P_sG+G\Delta f] \end{aligned} \tag{38}$$

The reaching dynamics can be expressed by

$$\dot{S}(t)=-P_sS(t)+G\Delta f \tag{39}$$

Therefore, the reaching dynamics is stable with Δf since $P_s>0$. The steady-state solution of Eq. (39) can be given as

$$S_{ss}=\int_0^t e^{-P_s(t-\tau)}G\Delta f\ d\tau \tag{40}$$

Hence, due to the nonideal effects, there is a steady-state error as $t\to\infty$ so that it cannot reach an equilibrium point. As a rule of thumb in sliding-mode controller design, it is possible to compensate the error by a large matrix P_s [2].

4. Application to SCOLE Model

The SCOLE system modeled by Meirovitch and Quinn (1987) is shown in Fig. 1 by accounting for bending and linear functions for axial and torsional deformations. A set of simultaneous nonlinear ordinary differential equations can be found in reference [10]. By using a perturbation approach, the

equations are separated into a set of equations for the rigid-body motions, representing zero-order effects, and a set of equations for the small elastic motions and deviations from the rigid-body motions, representing first-order effects. Their approach permits a maneuver strategy that is independent on the deflection control. Based on their formulation, a control scheme in Fig. 2 is designed with the OFC.

4.1 Elastic Tracking Model

A tracking model is presented to generate desired elastic states so that the natural deflection of a system is experienced. The structural equation of the SCOLE mast, for which the state estimator is designed with the assumption of the direct measurement of the rigid-body states, could be written as

$$\ddot{z}_f + C_{ff}\dot{z}_f + K_{ff}z_f = F_f - D_s(z_r, \dot{z}_f, \dot{z}_r, z_f) \tag{41}$$

where $D_s(z_r, \dot{z}_f, \dot{z}_r, z_f)$ is considered as a disturbance term including stiffening, gyroscopic, and coupled terms and the subscripts r and f stand for rigid-body and flexible-body, respectively.

The tracking model could be obtained from Eq. (41) by excluding time-varying matrices and internal forces so that the tracking model provides ideal elastic states to a controller. It serves as a nominal linear trajectory for a flexible-body dynamics. Using the modal analysis, the transformation between the tracking model and Eq. (41) is obtained by

$$z_f(t) = Tz_d(t) \tag{42}$$

where $T \in R^{l \times l}$ is an set of eigenvectors. The tracking model is expressed as

$$\ddot{z}_d(t) + 2\zeta\omega_n \dot{z}_d(t) + \omega^2 z_d(t) = -\mu T^{-1} A_e \ddot{\theta} \tag{43}$$

where A_e is defined as an influence matrix obtained by the terms of Eq. (41) associated with $\ddot{\theta}$ which will be the designed angular acceleration in numerical evaluation. The ζ and ω_n are the damping coefficient and the natural frequency, respectively. Hence, the right hand side [11] of the Eq. (43) is accounted for a tangential force associated with the desired angular displacement. The μ is a scaling factor which can be used in the case of a high angular velocity maneuver in order to operate the system within either an elastic range or a small deflection. The tracking model Eq. (43) is employed for the generations of the desired elastic states.

4.2 Start-Coast-Stop Maneuver Strategy

In the rigid-body like maneuver with the zero-order perturbation, the axis of rotation is not necessarily a principal axis so that the each moment along the $x_0y_0z_0$ axes of the zero-order perturbed moment M_0desired to produce a rigid-body rotation about one axis are obtained as

$$M_{01} = I_{11}\ddot{\theta} \tag{44}$$

$$M_{02} = I_{21}\ddot{\theta} - I_{31}\dot{\theta}^2 \tag{45}$$

$$M_{03} = I_{31}\ddot{\theta} + I_{21}\dot{\theta}^2 \tag{46}$$

where θ is the desired angular displacement. The inertia moments in the above equations are the elements of I_0, the mass moment of inertia, about the rotational axis. These moments are applied to the SCOLE to perform the slewing maneuver with respect to one axis. Instead of optimal formulation [11, 12] in order to minimize either operational time or fuel or both, which lead to solutions for two-point boundary problems, a simple operation is employed and targeted to the reduction of operational time and fuel consumption. A torque command input $M_{01} = u_c(t)$ for roll maneuver around x_0 axis in the paper used in conjunction with the input shaping technique is expressed as

$$u_c(t) = \begin{cases} T_{amp}\sin^2\Omega t & t \le t_0 = \frac{\pi}{\Omega} \\ u_c(t) = 0 & otherwise \end{cases} \tag{47}$$

where T_{amp} is the torque magnitude and Ω is the period of torque input profile. The input profile is used for start and stop motions. During the coasting period, no additional input is required except for control input to treat disturbances. The smooth input profile is selected because the excitation of high frequency modes should be reduced during the transient period.

In order to accurately arrive at the desired final angle of the roll maneuver, an analytical solution for intermediate time interval is needed. By taking time integration of Eq. (44) with Eq. (47), the desired coasting angular velocity is given as

$$\dot{\theta}_c = \frac{T_{amb}}{I_{11}}\left(\frac{t_0}{2} - \frac{\sin 2t_0}{4}\right) \tag{48}$$

where $\dot{\theta}_c$ is the costing angular velocity of $\dot{\theta}$. If the desired final angle θ_f is given, the coasting time interval, t_c, can be obtained as

$$t_c = t_0 + \frac{\theta_f}{\dot{\theta}_c} \tag{49}$$

4.3 Input Shaping

With the tracking model used to generate desired states for OFC, the input shaping technique [13] is employed to provide the residual vibration-free states after the end of input in an open-loop manner. Therefore, the system to be controlled is allowed to vibrate for one half period of the lowest mode. It is not necessary that the system should be held firmly to suppress the vibration on flexible structure in the case of rest-to-rest maneuver. With the two-impulse sequences, the shaped input u_s of desired input $u(t)$ could be written as

$$u_s(t) = A_1 u(t) + A_2 u(t - \Delta T) \tag{50}$$

in which

$$A_1 = \frac{1}{1 + K_p}$$

$$A_2 = \frac{K_p}{1 + K_p}$$

$$K_p = e^{-\zeta\pi/\sqrt{1-\zeta^2}}$$

$$\Delta T = \frac{\pi}{\omega_n\sqrt{1-\zeta^2}}$$

where ω_n and ζ are vibration modal frequency and damping, respectively of a second-order modal equation. This function as a true maneuver input is applied to the tracking model and the shuttle operation of SCOLE system for a large angle maneuver.

4.4 Numerical Simulation

The full-order model, 84 degrees of freedom, is reduced to 12 degrees of freedom including 6 rigid-body modes by using the frequency dependent Krylov vectors [14] to design the OFC. The proportional damping formula is used as $C_r = \alpha M_r + \beta K_r$ where $\alpha = \beta = 0.005$ were selected, but we know that the damping factor of space structures is very small so that the zero damping case is discussed at the end of the section. The M_r and K_r are the reduced mass and stiffness matrices of the SCOLE mast. The first and second natural frequencies of the mast are 0.9563 Hz and 1.0221 Hz, respectively.

For the application of the OFC to the SCOLE model, Eq. (15) is expressed with the assumption of the measurable rigid-body states as

$$u(t) = -(GB)^{-1}[G(A - K_f C)\hat{z}(t) + P_s G z_c(t) + xGz_{rc}(t) + GK_p y(t) + GD\dot{y}(t) - G\dot{z}^{\times}(t)] \tag{51}$$

where an attitude error feedback term $xGz_{rc}(t)$ is

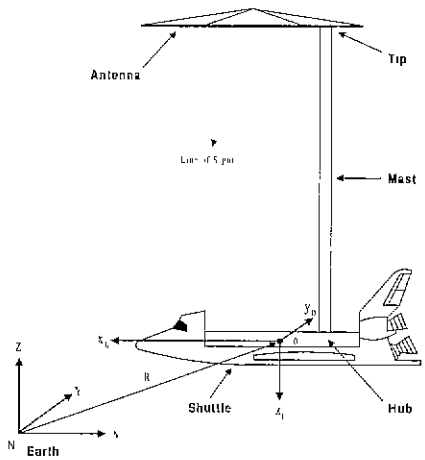

Fig. 1 Spacecraft Control Laboratory Experiment Configuration

introduced which will be necessary for the shuttle control. The $z_{rc}(t)$ is only the rigid-body state error.

There are 3 torque and 3 force actuators applied for the control of the shuttle. The 3 torque wheels are mounted at the mast-tip to control vibration. In this study, it is assumed that the measured variables are θ, $\dot{\theta}$, x, and $\dot{x}$ of the shuttle. The state variables of the mast with respect to the shuttle are estimated by the Kalman filter using 3 displacement (x, y and z) and 3 velocity ($\dot{x}$, $\dot{y}$ and $\dot{z}$) sensors mounted at the mast-tip. The configuration of the actuators and sensors is collocated at both the shuttle and the mast-tip.

Several design parameters are tabulated in Table 1 for the output feedback controller. The optimal

weighting matrix is selected as

$$Q_s = \begin{bmatrix} \rho_i I^{6\times 6} & 0 \\ 0 & \rho_i \omega_i^2 \end{bmatrix} \quad (52)$$

where $i = 1, \cdots \ell$ and ℓ is the same as the order of the estimator. For the state estimation, it is initially assumed that the disturbances caused primarily by tangential and centrifugal forces are known in the controller and estimator design. In the stage of evaluating the performance of the output feedback controller, the disturbance terms are dropped in both the controller and estimator, but the time-varying effects on the system matrices such as stiffening and gyroscopic terms remain
in only the estimator dynamics. In the case of slower angular motion, the stiffening and gyroscopic effects are smaller.

Table 1 Design Parameters for Controller and Estimator

Rigid−Body Feedback Coefficient	χ	1000
Global Reaching Coefficient	ν	20
Scaling Factor	μ	1
Influence Factor	A_e	$I^{\ell\times\ell}$
Rigid−Body Weighting	Q_b	$10^{-3} I^{\ell\times\ell}$
Measurement Noise	Q_m	$10^{-4} I^{\ell\times\ell}$
Input Torque Period	Ω	4 *rad*/sec

The influence term of the tracking model in Eq. (43) adopted the tangential force which can provide the effect of the angular acceleration of the shuttle in the specific application to the SCOLE model. Of course, the influence term depends on a specific problem such that a designer could select a different one. During the numerical simulation, the first two modes are most significantly excited by the shaped input command in an open-loop manner. In order to obtain no residual vibration, the 2nd mode frequency of the tracking model is replaced with the 1st mode frequency because only the 1st mode is used for shaping the input. Therefore, the tracking model does generate four non-zero states and maintain the remaining states at zero.

The desired input command is shaped by a two-impulse sequence. Of course, more impulses can be used for the increment of robustness as well as the reduction of residual vibration. However, the control suffers from longer operational time. Furthermore, there is a drawback of input shaping technique in on-line implementation of multiple impulse sequence. It is difficult to design the amplitudes of 2nd impulse, 3rd impulse, and so on according to estimated natural frequencies. For a instance, Tzes [15] used only two-impulse sequence for the application of a single link arm to pick a payload by estimating the first natural frequency in frequency domain. In this paper, the on-line operation of the input shaping technique is not implemented. However, it is pursued to give a faster operation, a more efficient maneuver, and a more reliable controller in a realistic problem.

All computations and plots shown in the paper were performed on an IBM RISC 6000 Workstation. The control schematic diagram which indicates the interactions among the commands, ideal model, sliding-mode controller, SCOLE simulation, and state estimation is shown in Fig. 2.

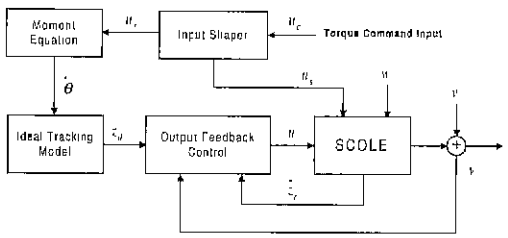

Fig. 2 Closed-Loop Control System

In the numerical simulation, four cases are compared from the aspect of the antenna deflections and rotations. The four cases are

Case 1. Tracking Control (a) requires that most nonideal effects are assumed to be known for the design of the OFC and time-varying Kalman filter However, the OFC does not include the time-varying effects such as stiffening and gyroscopic terms. The OFC attempts to follow the states of the ideal tracking model. The control efficiency is demonstrated by this case.

Case 2. Tracking Control (b) allows the most significant disturbances in the slewing maneuver to be dropped in the design of the OFC and time-varying Kalman filter out of the Tracking Control (a) case. The disturbances are the tangential and centrifugal forces The OFC again tracks the states of the ideal tracking model. The robustness of the OFC is

illustrated by this case.

Case 3. Open-Loop Control in that neither the OFC nor Kalman filter is involved. The input shaping technique is used to evaluate the performance with only two-impulse sequence.

Case 4. Rigid-Body Control in that the ideal tracking model is not used. The OFC is attempting to hold the flexible mast like a rigid-body.

In the four cases, the input command with the magnitude $T_{amp}=20\ lb\cdot ft(2.7651\ Kg_f\cdot m)$ in Fig. 3 is shaped by a two-impulse sequence and then is applied to the shuttle for a 30 ° roll maneuver. The output feedback controller is charged with rejecting perturbations during the entire slewing motion. The desired motion of the shuttle is shown in Fig. 4 with the maximum velocity around 6 deg/sec

The main control objective of the SCOLE model is to aim the antenna within a certain tolerance 0.02 in short time. Hence, plots of the antenna rotations versus time are presented. Figs. 5 to 7 illustrate the instantaneous antenna rotations with

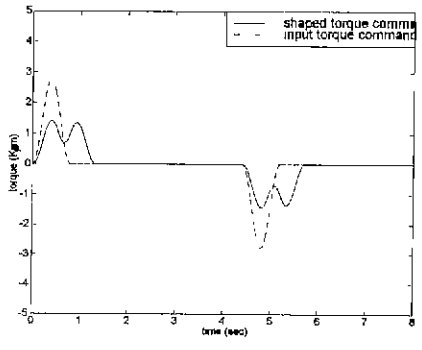

Fig. 3 Command Inputs for 30 ° Roll Maneuver

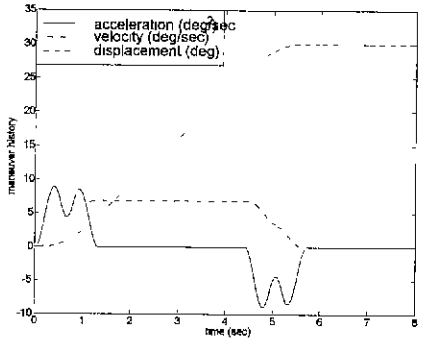

Fig. 4 Maneuver Strategy of the Shuttle for 30 ° Roll Maneuver

respect to $x_0y_0z_0$ axes, respectively.

The figures show the responses produced during the maneuver with all four of the control techniques. The effect of the tangential and centrifugal terms in the controller and estimator in the case of tracking control (b) shows more angular displacement and takes a longer time than the one of tracking control (a) to settle down the oscillatory deflection because the OFC is employing a globally asymptotic reaching technique [2] unlike a rapid switching technique. Nevertheless, it does eventually and quickly damp out the residual oscillatory deflection of all axes in the presence of modeling errors in the tracking control (a).

The equation of control effort $C.E.$ for Fig. 8 and 9 is defined as

$$C.E.=\int_0^{\infty} u(t)^T u(t)dt \tag{53}$$

The rigid-body control is not very effective in controlling the vibration compared to the *tracking control (a)*.

The *tracking control (b)* requires more control effort than two other cases, and after 6 sec, continuously consumes energy in order to damp out the residual vibration. The *tracking control (a)* consumes the least amount of control effort and accomplishes the 30 maneuver. The control effort for the entire system operation in the *tracking control (a)* is a small quantity below $5(lb\cdot ft)^2(0.4781 Kg_f\cdot m)$ which can be indirectly comparable to the results of Meirovitch and Quinn (1987). They used either distributed force actuators or 10 discrete force actuators in controlling the vibration

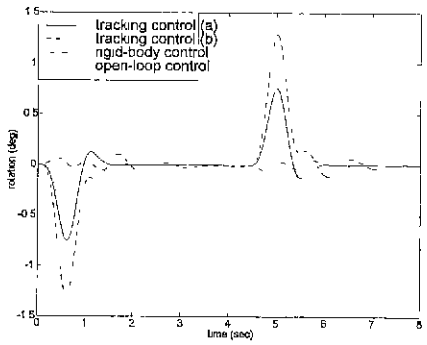

Fig. 5 Antenna Rotation about x_0 during a 30 ° Maneuver

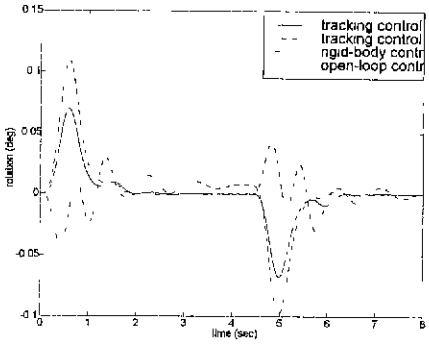

Fig. 6 Antenna Rotation about y_0 during a 30 ° Maneuver

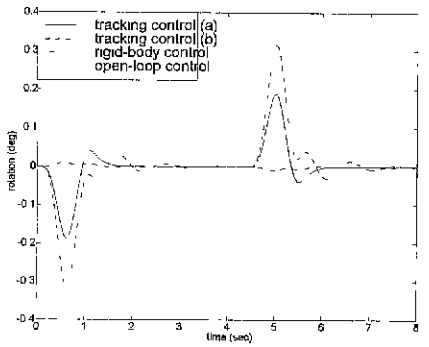

Fig. 7 Antenna Rotation about z_0 during a 30 ° Maneuver

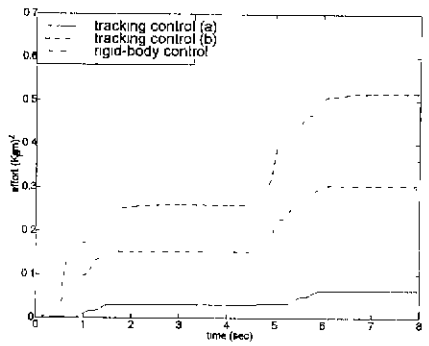

Fig. 8 Torque Control Efforts during a 30 ° Maneuver

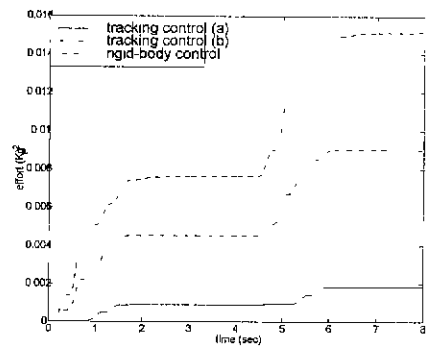

Fig. 9 Force Control Efforts during a 30 ° Maneuver

of mast instead of using torque wheel actuators in this paper. Each *C.E.* is for the entire operational effort.

The *Tracking control (a)* is tested for the zero damping case $C=0$ with the same design paramters in Table 1. It turns out that the residual vibration of the mast exists after the end of the 30 ° slewing maneuver. However, the maximum vibration amplitude is below 0.02 ° which is the control objective of the SCOLE operation. It appears that the overall performance of the OFC is similar to the non-zero damping case.

5. Conclusions

The OFC is developed for a linear stochastic system with known disturbance. The error states are determined using the Kalman filter to define the number of sliding hypersurfaces. The number of controller poles results from the thickness of boundary layers and the remaining poles for the entire states are determined by the sliding hypersurface selection. The OFC minimizes the expected value of a guadratic objective function composing of error states which always remain on the intersection of sliding hypersurfaces with respect to the remaining poles.

In the numerical simulation with the SCOLE model, the OFC is modified for the maneuver of the rigid-body and combined with the ideal tracking model and the input shaping. The first-mode tracking strategy is shown to be more efficient than the rigid-body motion strategy. With the limited actuators and sensors at the mast-tip, the large angle maneuver is successfully accomplished without significant residual vibration.

References

1. J. E. Slotine, "The Robust Control of Robot

Manipulators," Journal of Robotics Research, 4, 49-64, 1985.
2. O. Mostafa and H. Oz, "Chatter Elimination in Variable Structure Control Maneuvering of Flexible Spacecraft," Journal of the Astronautical Sciences, 37, 529-550, 1989.
3. H. Oz and O. Mostafa, "Variable Structure Control System(VSCS) Maneuvering of Flexible Spacecraft," Journal of the Astronautical Sciences, 36, 311-344, 1988.
4. N. K. Gupta, "Frequency-Shaped Cost Functionals: Extension of Linear-Quadratic-Gaussian Design Methods," Journal of Guidance, Control and Dynamics, 3, 529-535, 1980.
5. A. Sinha and D. W. Miller, "Optimal Sliding-Mode Control of a Flexible Spacecraft under stochastic disturbance," Journal of Guidance, Control, and Dynamics, 18, 486-492, 1995.
6. V. I. Utkin, Sliding Modes in Control Optimization, Springer-Verlag, New York, 1992.
7. K. D. Young and U. Ozguner, "Frequency Shaping Compensator Design for Sliding Mode," Journal of Control, 57, 1005-1019, 1993.
8. C. Edwards and S. K. Spurgeon, Sliding Mode Control: Theory and applications, Taylor & Francis Inc., PA., 1998.
9. W. L. Brogan, Mordern Control Theory, Prentice-Hall Inc., New Jersey, 1991.
10. L. Meirovitch and R. D. Quinn, R. D., " Maneuvering and Vibration Control of Flexible Spacecraft," Journal of the Astronautical Sciences, 35, 301-328, 1987.
11. C. J. Swigert, "Shaped Torque Technique," Journal of Guidance, Control, and Dynamics, 3(5), 460-467, 1980.
12. J. L. Junkins and J. D. Turner, "Optimal Spacecraft Rotational Maneuvers", Elsevier Science Publishers, New York, 1986.
13. N. C. Singer and W. P. Seering, "Preshaping Command Inputs to Reduce System Vibration," Journal of Dynamic Systems, Measurement, and Control, 112, 76-82, 1990.
14. Y.-G. Sung and Y.-P. Park, "Model Reduction of Semi-Positive Definite Systems Reflected to Actuator and Sensor Locations," KSME International Journal, 13, 714-726, 1999.
15. A. P. Tzes, Self-Tuning Controllers for Flexible Link Manipulators, Ph.D. Thesis, Ohio State University, Columbus, OH., 1990.